Journal of Inorganic Biochemistry 192 (2019) 119–125

Contents lists available at ScienceDirect

Journal of Inorganic Biochemistry

journal homepage: www.elsevier.com/locate/jinorgbio

Functionalization of luminescent lanthanide-gallium metallacrowns using copper-catalyzed alkyne-azide cycloaddition and thiol-maleimide Michael addition

Jacob C. Lutter, Beatriz A. Lopez Bermudez, Tu N. Nguyen[1], Jeff W. Kampf, Vincent L. Pecoraro*

Willard H. Dow Laboratories, University of Michigan, 930 N. University Ave., Ann Arbor, MI, USA

ARTICLE INFO

Keywords:
Lanthanide ions
Metallacrowns
Supramolecular chemistry
Alkyne-Azide coupling
Michael coupling
Luminescence

ABSTRACT

The synthesis and characterization of $\{Ln[12\text{-}MC^{III}_{GaN(eshi)}\text{-}4]\}_2(iph)_4$ and $\{Ln[12\text{-}MC^{III}_{GaN(shi)}\text{-}4]\}_2(miph)_4$ metallacrowns (MCs), where shi^{3-} is salicylhydroximate, $eshi^{3-}$ is 4-ethynylsalicylhydroximate, iph^{2-} is isophthalate, and $miph^{2-}$ is 5-maleimidoisophthalate, is reported. The ethynyl functionality allows for coupling of MCs to azides using copper(I) catalyzed alkyne-azide cycloaddition (CuAAC), while the maleimido functionality allows for coupling of the MCs to thiol-bearing compounds. We demonstrate these coupling reactions using benzyl azide for the former and cysteamine for the latter, with complete conversion shown by ESI-MS. With the Sm analogues, the MCs exhibit characteristic luminescent emission of Sm(III), which is preserved after introducing the ethynyl and maleimido groups onto the MC scaffold. Furthermore, the high stability of these compounds in solution illustrates that once functionalized, the MCs are promising for fluorescent imaging applications.

1. Introduction

Metallacrowns (MCs) were introduced by Pecoraro and Lah as inorganic structural analogs to organic crown ethers in 1989 [1]. Since their discovery, this class of coordination complexes has been involved in a wide variety of topics including host guest binding [2–5], molecular magnetism [6–9], coordination polymers [10–12], magnetic resonance imaging contrast [13,14], and lanthanide luminescence [15–21]. Each of these fields have seen rather interesting developments [22–25], but for the purpose of this study the focus will be on lanthanide based luminescence. Lanthanide(III) ions have attractive properties for use in optical imaging, such as long lifetimes, narrow characteristic emission, and photobleaching resistance [26,27]. However, an f-f excitation is Laporte forbidden resulting in low molar absorptivity ($\varepsilon < 10\,M^{-1}\,cm^{-1}$) and low luminescence intensity; therefore, an organic antenna ($\varepsilon \sim 10^4$–$10^5\,M^{-1}\,cm^{-1}$) is often employed to efficiently absorb light and transfer the absorbed energy from its excited state to the emitting levels of the lanthanide ion [27]. Metallacrowns and related metallacryptates have been reported as excellent antenna for lanthanide sensitization [15–18,21], some of which work very well with near infrared (NIR) Ln^{3+} ions and are able to fix and image necrotic HeLa cells selectively [19,20].

To broaden the application of these excellent lumiphores for both *in vitro* and *in vivo* applications, one needs to develop methods to functionalize the periphery of metallacrowns. One attractive approach is that of "click" chemistry, which should allow appending a wide variety of useful molecules ranging from targeting agents to antennae, without disrupting the self-assembled core of the metallacrown. The concept of "click" chemistry was introduced by K. Barry Sharpless in 2001 [28]. Formally, he defined a "click" reaction as a C-X-C bond (X is a heteroatom) forming reaction with a large driving force (> 20 kcal/mol). The reaction should also have a wide scope for coupling partners and have easily isolable products in benign solvents such as water. The scope of reactions that falls under "click" chemistry include cycloaddition reactions, nucleophilic ring opening reactions, carbonyl chemistry towards formation of stable products such as ureas or amides, and addition to carbon-carbon multiple bonds (such as a Michael addition).

One "click" reaction of interest for this work is the copper-catalyzed alkyne azide [3 + 2] cycloaddition (CuAAC). Originally called the Huisgen coupling reaction, this reaction combines an alkyne and an azide to form a 1,4 substituted triazole, but was limited as it required energy input in the form of heat [29]. In 2001, Meldal and Sharpless

* Corresponding author.
E-mail address: vlpec@umich.edu (V.L. Pecoraro).
[1] Present Address: Laboratory of Molecular Simulation, Institut des sciences et ingénierie chimiques (ISIC), Ecole polytechnique fédérale de Lausanne (EPFL Valais), Rue de l'Industrie 17, 1951 Sion, Switzerland.

https://doi.org/10.1016/j.jinorgbio.2018.12.011
Received 2 October 2018; Accepted 21 December 2018
Available online 23 December 2018
0162-0134/

independently discovered that the addition of copper(I) to this system greatly catalyzes the cycloaddition and allows one to work at ambient temperatures [28,30]. In addition, the inclusion of copper(I) chelators such as tris[(benzyl-1,2,3-triazolyl)methyl]amine (TBTA) can also improve the yield and rate of the reaction and opened up the possibility of its use in bioconjugation [31]. The mechanism for the copper catalyzed cycloaddition is not fully understood, but based on kinetic studies the reaction appears to be second order in both the copper catalyst and alkyne, which suggests that the intermediate species has a ratio of 2 copper(I) to 2 alkyne to one azide [30]. The most likely mechanism which includes this ratio was proposed by Meldal in 2008. Despite the complexity of this reaction, the results are rather straightforward and the CuAAC has found use across pharmaceutical and biochemical communities.

The other "click" reaction employed in this work is the Michael addition between thiols and maleimides. This reaction is driven by the withdrawing effects of the carbonyl groups along with the enhanced reactivity of the alkene site due to ring strain [32]. The thiol-maleimide coupling reaction results in the formation of a stable thioether bond that cannot be cleaved by reducing agent; additionally, this reactions occurs rapidly at neutral or slightly acidic conditions, which is a notable advantage for biological applications [33,34]. The mechanism of thiol-maleimide coupling is typically described a Michael-type addition with three possible pathways: *i*) a thiolate-catalyzed addition of a thiol to a maleimide; *ii)* formation of thiolate anions from acid-base equilibrium reactions; and lastly; *iii)* formation of thiolate anions following a nucleophilic-initiated mechanism [32,35]. Due to the mild reaction conditions, rapid and high reactivity, and selectivity, thiol-maleimide Michael "click" conjugation reactions have become a popular and reliable method of bioconjugation, and more recently a promising tool in polymer and material synthesis [32].

To incorporate the use of CuAAC and thiol-maleimido coupling onto the metallacrown archetype, an alkyne functionality was added onto the salicylhydroximate (shi^{3-}) and a maleimido functionality was included on the isophthalate (iph^{2-}). Rentschler and coworkers have previously reported a salicylhydroxamic acid derivative (H_3eshi) in 2015 which features an ethyne in the fourth position [36]. While that work was focused on coupling azides of interest for magnetic study of copper 12-MC-4 s, this same ligand could be of use with gallium metallacrowns which have lanthanide based luminescence, such as the {Ln[12-$MC^{III}_{GaN(shi)}$-4]}$_2$(iph)$_4$ metallacrown reported by Pecoraro and coworkers in 2018 [18]. This metallacrowns not only features excellent lanthanide photophysical properties, but also demonstrates a wide range of lanthanide emission. These features could be useful towards the development of color coding biological assays if these complexes could be functionalized with appropriate biological markers. In addition, the use of the thiol-maleimido Michael addition is employed *via* introduction of a used in the previously reported structure. The first steps towards such a goal is reported herein as the coupling of these lanthanide/gallium 12-MC-4 dimer complexes to small molecules such as benzyl azide or cysteamine.

2. Experimental

2.1. Synthetic procedures

2.1.1. Methyl 4-ethynylsalicylate

Methyl 4-ethynylsalicylate was synthesized by modifying a literature procedure [36]. Thirty-six mmol (10.01 g, 1 equiv.) of methyl 4-iodosalicylate was dissolved in 180 mL of triethylamine to form a clear and brown solution. Then, 43.2 mmol (6.15 mL, 1.2 equiv.) of trimethylsilylacetylene was added and stirred. Next, 1.8 mmol (1.2763 g, 0.05 equiv.) of palladium(II) bis(triphenylphosphine)dichloride and 3.6 mmol (0.6855 g, 0.1 equiv.) of copper(I) iodide was added and stirred for 24 h to form a cloudy brown-green solution. The reaction was quenched by adding 145 mL of 1 M aqueous ammonium chloride and stirring for about a half hour. This solution was extracted using two 100 mL portions of ethyl acetate, then another three 50 mL portions, and dried over sodium sulfate and gravity filtered. The filtrate was evaporated on a flash evaporator to give a brown-red oil. The residue was dissolved in 10 mL of dichloromethane and purified using a silica gel column with an increasing gradient of dichloromethane in hexanes to yield a yellow oil. The purified intermediate was dissolved in 45 mL of tetrahydrofuran and treated with 45 mL of 1 M tetrabutylammonium fluoride in tetrahydrofuran for 2 h. The resulting honey-colored mixture was acidified to pH 1 using 1 M aqueous hydrochloric acid, then mixed with 50 mL of distilled water. The mixture was extracted with four portions of ethyl acetate, dried over sodium sulfate and gravity filtered. The filtrate was evaporated on a flash evaporator to yield methyl 4-ethynylsalicylate as a yellow powder. The synthetic yield was 87%. Elemental analysis of $C_{10}H_8O_3$ [fw = 176.17 g/mol] % found (calculated): %C 67.92 (68.18); %H 4.59 (4.58); %N 0.00 (0.00). ^{1}H NMR (400 MHz, d_6-DMSO) δ (ppm): 10.54 (1H, s), 7.75 (1H, d), 7.07 (1H, d), 7.02 (1H, dd), 4.45 (1H, s), 3.88 (3H, s).

2.1.2. 4-ethynylsalicylhydroxamic acid (H_3eshi)

H_3eshi was synthesized by modifying a literature procedure [36]. First, 31.22 mmol of methyl 4-ethynylsalicylate (5.50 g, 1 equiv.) was suspended in 150 mL of methanol. Separately, 93.66 mmol of hydroxylamine hydrochloride (6.51 g, 3 equiv.) and 124.88 mmol of potassium hydroxide (8.24 g, 4 equiv.) were dissolved in 150 mL of methanol to form clear and colorless solutions. The hydroxylamine hydrochloride and potassium hydroxide solutions were combined, and a colorless potassium chloride precipitate was observed. The mixture was left to stir for 10 min, then the potassium chloride was vacuum filtered from a clear and colorless filtrate. This filtrate was combined with the suspension of methyl 4-ethynylsalicylate to form a clear and orange solution. This solution was stirred for 24 h. Next, another set of hydroxylamine hydrochloride and potassium hydroxide solutions in 150 mL of methanol were prepared, combined and filtered as described previously to obtain another clear and colorless filtrate. This filtrate was combined into the reaction solution and let stir for another 24 h. The solution was evaporated down to approximately 100 mL using a flash evaporator and acidified to a pH 1 using 1 M hydrochloric acid. Then 500 mL of distilled water was added followed by 200 mL of brine. This solution was extracted with ten portions of ethyl acetate, dried over sodium sulfate and gravity filtered. The filtrate was evaporated using a flash evaporator to a yellow powder, which was triturated for 20 min in 75 mL of dichloromethane. The cloudy mixture was vacuum filtered to yield 4-ethynylsalicylhydroxamic acid as a yellow powder. The synthetic yield was 85%. Elemental analysis for $C_9H_7NO_3{\cdot}0.15H_2O$ [179.86 g/mol] % found (calculated): %C 60.22 (60.10); %H 4.16 (4.09); %N 7.81 (7.79). ^{1}H NMR (400 MHz, d_6-DMSO) δ (ppm): 12.25 (1H, s), 11.42 (1H, s), 9.39 (1H, s), 7.66 (1H, d), 6.98 (1H, s), 6.96 (1H, d), 4.35 (1H, s).

2.1.3. 5-(3-carboxylacrylamide)isophthalic acid

5-(3-carboxylacrylamide)isophthalic acid was synthesized by modifying a literature procedure [37]. First, 100 mmol of 5-aminoisophthalic acid hydrate (19.92 g, 1 equiv.) and 110 mmol of maleic anhydride (10.79 g, 1.1 equiv.) were dissolved in 200 mL of DMF. The mixture was stirred for ~ 6 h after which DMF was removed under vacuum. The obtained product was washed with acetone to give 5-(3-carboxyacrylamide)isophthalic acid as a yellow powder. The synthetic yield was 68%. Elemental analysis for $C_{12}H_9NO_7$. 0.2 DMF. 0.8 H_2O [308.23 g/mol] % found (calculated): %C 49.09 (49.10); %H 4.13 (3.92); %N 5.33 (5.45). ^{1}H NMR (400 MHz, d_6-DMSO) δ (ppm): 13.20 (1H, s), 11.08 (1H, s), 10.38 (1H, s), 8.16 (1H, d), 7.67 (1H, dd), 6.96 (1H, d), 6.46 (1H, d), 6.31 (1H, d).

2.1.4. 5-maleimidoisophthalic acid (H_2miph)

5-maleimidoisophthalic acid was synthesized according to a known

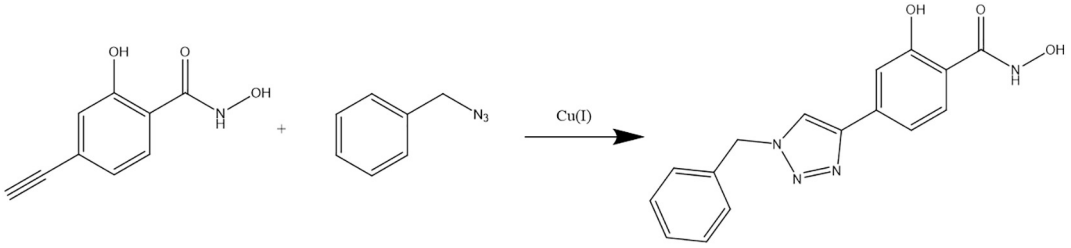

Scheme 1. CuAAC of H_3eshi and benzyl azide as a route to functionalize a metallacrown.

procedure [37]. First, 10.0 mmol of 5-(3-carboxyacrylamide)isophthalic acid (2.79 g, 1 equiv.) was added in to the solution of 15.0 mL acetic anhydride with 5.0 mmol sodium acetate trihydrate (0.68 g, 1 equiv.). The resulting mixture was stirred at 60 °C for 2.5 h. Acetic anhydride was then removed under vacuum and water (20.0 mL) was added. The slurry mixture was stirred at 70 °C for another 2 h, filtered, and washed with copious amount of water. The white solid obtained is dried under vacuum to give pure 5-maleimidoisophthalic acid. The synthetic yield was 77%: Elemental analysis for $C_{12}H_7NO_6$ [261.19 g/mol] % found (calculated): %C 55. 10 (55.18), %H 2.71 (2.70), %N 5.48 (5.36). ^{1}H NMR (400 MHz, d_6-DMSO) δ (ppm) 8.49 (1H, s), 8.18 (2H, s), 7.24 (2H, s).

2.1.5. Tris(benzyltriazolylmethyl)amine, *TBTA*

TBTA was synthesized by modifying literature procedure for CuAAC in H_2O/t-butanol [30]. One mmol of tripropargylamine (142 µL, 1 equiv.) and 3 mmol of benzyl azide (375 µL, 3 equiv.) were dissolved in 12 mL of a 1:1 H_2O:t-butanol mixture. Next, 0.03 mmol of sodium L-ascorbate was added as a 1 M solution in H_2O (300 µL, 0.03 equiv.), followed by 0.03 mmol of copper(II) sulfate as a 3 M solution in H_2O (100 µL, 0.03 equiv.). This mixture was allowed to react for 3 days, then was dissolved in 50 mL of cold H_2O. This mixture was then extracted with five portions of 25 mL of ethyl acetate. The organic layers were combined, dried over sodium sulfate, then gravity filtered. The filtrate was evaporated using a flash evaporator, then redissolved in 5 mL of DMF. The solution was evaporated using a flash evaporator to give TBTA as a brown powder. The synthetic yield was 88%. Elemental analysis for $C_{30}H_{30}N_{10}$. 1.25 $C_4H_{10}O$ [fw = 623.04 g/mol] % found (calculated): %C 67.45 (67.47). %H 6.49 (6.84), %N 22.49 (22.48). ^{1}H NMR (400 MHz, d_6-DMSO): 8.09 ppm (3H, s), 7.32 ppm (15H, m), 5.59 (6H, s), 3.61 (6H, s).

2.1.6. General synthesis for {Ln[12-$MC^{III}_{GaN(eshi)}$-4]Na}$_2$(iph)$_4$, ***Ln-e8***

Ln-e8 were synthesized by modifying a literature procedure [18]. 0.125 mmol of $Ln(NO_3)_3.xH_2O$ (Ln = Sm or Y, 1 equiv.) and 0.6 mmol of $Ga(NO_3)_3$ (0.1535 g, 4.8 equiv.) were dissolved in 5 mL of DMF. Separately, 0.6 mmol of H_3eshi (0.1063 g, 4.8 equiv.), 0.3 mmol of isophthalic acid (0.0498 g, 2.4 equiv.), and 2.4 mmol of saturated aqueous sodium hydroxide (119.4 µL, 19.2 equiv.) were dissolved in 15 mL of DMF for form a clear and yellow solution. The solutions were combined and let stir for at least 1 h, then gravity filtered. The filtrate was evaporated slowly over 2–4 weeks yielding yellow-brown crystalline plates, isolated by vacuum filtration and washing with cold DMF.

2.1.7. Sm_2Ga_8(eshi)$_8$(iph)$_4Na_2$(DMF)$_{15}$(H_2O)$_8$, ***Sm-e8***

The synthetic yield was 10% based on samarium nitrate hexahydrate. Elemental analysis for $Sm_2Ga_8C_{149}H_{169}N_{23}O_{63}Na_2$ [fw = 4194.57 g/mol] % found (calculated): %C 42.73 (42.67); %H 4.00 (4.06); %N 7.87 (7.68). ESI-MS for $Sm_2Ga_8C_{104}H_{48}N_8O_{40}$ $[M]^{2-}$, found (calculated): 1454.19 (1456.22). ^{1}H NMR (500 MHz, d_4-MeOH): 8.66 ppm (3H, s), 8.08 ppm (2H, d), 7.56 ppm (1H, t), 7.13 ppm (2H, s), 6.88 ppm (2H, d), 3.49 ppm (2H, s).

2.1.8. Y_2Ga_8(eshi)$_8$(iph)$_4Na_2$(DMF)$_{16}$(H_2O)$_{12}$, ***Y-e8***

The synthetic yield was 11% based on yttrium nitrate hexahydrate. Elemental analysis for $Y_2Ga_8C_{152}H_{184}N_{24}O_{68}Na_2$ [fw = 4216.82 g/mol] % found (calculated): %C 41.72 (41.73); %H 3.19 (3.17); %N 6.05 (6.08). ESI-MS for $Y_2Ga_8C_{104}H_{48}N_8O_{40}$ $[M]^{2-}$, found (calculated): 1395.58 (1392.11). ^{1}H NMR (500 MHz, d_4-MeOH): 9.07 ppm (1H, s), 8.23 ppm (2H, d), 8.03 ppm, (2H, d), 7.30 ppm (1H, t), 7.09 ppm (2H, s), 6.85 ppm (2H, d), 3.47 ppm (2H, s).

2.1.9. CuAAC on ***Sm-e8*** Metallacrowns to make the benzyl triazyl species ***Sm-bt8***

To obtain a **Sm-e8** with all eight functionalities reacted with an azide, a modified literature procedure was used [36]. First, 6.65 µmol of TBTA (4.14 mg, 0.525 equiv.), 13.3 µmol of CuI (2.54 mg, 1.05 equiv.), and 13.3 µmol of sodium ascorbate (2.63 mg, 1.05 equiv.) were dissolved in 1 mL of DMSO. Next, 114 µmol of benzyl azide (14.28 µL, 9 equiv.) followed by 12.7 µmol of **Sm-e8** (50.00 mg, 1 equiv.) were added and the reaction was warmed to 75 °C and stirred for 24 h. The solution was allowed to evaporate slowly in a humid environment until a grey powder formed. This powder was isolated *via* vacuum filtration and washing with cold water. Elemental analysis shows that TBTA precipitates along with the clicked metallacrown. The synthetic yield was 70%. Elemental Analysis for $Sm_2Ga_8C_{160}H_{104}N_{32}O_{40}Na_2$. TBTA. 14 DMSO. H_2O [fw = 5661.72 g/mol] % found (calculated): %C 46.22 (46.25), %H 4.03 (3.92), %N 10.25 (10.39). ESI-MS for $Sm_2Ga_8C_{160}H_{104}N_{32}O_{40}$ $[M]^{2-}$, found (calculated): 1986.94 (1988.48) (Scheme 1).

2.1.10. General synthesis for {Ln[12-$MC^{III}_{GaN(shi)}$-4]Na}$_2$(miph)$_4$, ***Ln-m4***

First, Ln[12-$MC^{III}_{GaN(shi)}$-4]($C_7H_5O_2$)$_4$(C_5H_6N) metallacrowns were synthesized according to a literature procedure [17]. Then 0.5 mmol (1 equiv.) of metallacrown with Ln = Sm or Y was dissolved in 5–10 mL of DMF with 1.00 mmol of H_2miph (0.26 g, 2 equiv.) and stirred for 6 h. The DMF was evaporated using a vacuum, and the powder obtained was washed with methanol to yield pure product.

2.1.11. Sm_2Ga_8(shi)$_8$(miph)$_4Na_2$(CH_3OH)$_3$(H_2O)$_{19}$, ***Sm-m4***

The synthetic yield was 81% based on metallacrown. Elemental Analysis for $Sm_2Ga_8C_{170}H_{102}N_{12}O_{70}Na_2$ [fw = 3580.49 g/mol] % found (calculated): %C 35.94 (35.89), %N 2.84 (2.89), %H 4.76 (4.69). ESI-MS for $Sm_2Ga_8C_{104}H_{52}N_{12}O_{48}$ $[M]^{2-}$, found (calculated): 1547.73 (1550.22). ^{1}H NMR (400 MHz, d_6-DMSO) δ (ppm): 8.33 (m, 1H), 7.95 (broad s, 2H), 7.51 (td, 2H), 7.20 (d, 2H), 6.91 (broad s, 2H), 6.71 (broad s, 2H), 5.46 (broad s, 2H).

2.1.12. Y_2Ga_8(shi)$_8$(miph)$_4$(C_5H_6N)$_2$(C_5H_5N)$_2$(CH_3OH)(C_3H_7NO)$_2$(H_2O)$_{12}$, ***Y-m4***

The synthetic yield was 84% based on metallacrown. Elemental Analysis for $Y_2Ga_8C_{131}H_{116}N_{18}O_{63}$ [fw = 3686.03 g/mol] % found (calculated): %C 42.63 (42.69), %N 3.07 (3.17), %H 6.85 (6.84). ESI-MS for $Y_2Ga_8C_{104}H_{52}N_{12}O_{48}$ $[M]^{2-}$, found (calculated): 1486.70 (1486.21). ^{1}H NMR (400 MHz, d_6-DMSO) δ (ppm): 8.96 (d, 1H), 8.04 (d, 2H), 7.87 (t, 2H), 7.22 (t, 2H), 7.07 (s, 2H), 6.87 (t, 2H), 6.69 (t, 2H).

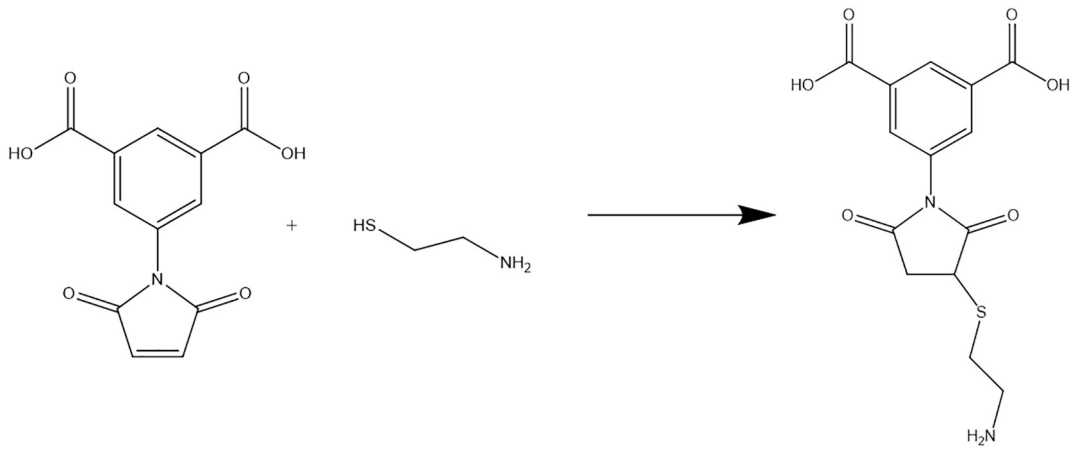

Scheme 2. Micheal addition of H_2miph and cysteamine as a route to functionalize a metallacrown.

*2.1.13. Thiol Michael Addition on **Sm-m4** Metallacrowns to make the thioether **Sm-te4***

Sm-m4 (0.020 mmol) and cysteamine (0.18 mmol) were mixed in 2 mL DMF. After 4 h, DMF was evaporated under vacuum and the obtained powder was washed with methanol to give the pure product. The synthetic yield was > 95%. Elemental Analysis for $Sm_2Ga_8C_{116}H_{148}N_{16}O_{78}S_4Na_2$ [fw = 4047.22 g/mol] % found (calculated): %C 34.38 (34.43), %H 3.56 (3.69), %N 5.45 (5.54). ESI-MS for $Sm_2Ga_8C_{112}H_{80}N_{16}O_{48}S_4$ $[M]^{2-}$, found (calculated): 1702.18 (1704.28) (Scheme 2).

2.2. Physical methods

ESI-QTOF MS was performed on an Agilent 6520 Accurate-Mass Q-TOF LC/MS quadrupole time of flight mass spectrometer in negative ion mode with a fragmentation voltage of 250 V. Samples were prepared by dissolving approximately 1 mg of compound in 1 mL of methanol, then diluting 20 µL of the solution into another 1 mL of methanol. Samples were directly injected using a syringe (without the HPLC or autosampler). Data were processed with Agilent MassHunter Qualitative Analysis software. Elemental analysis was performed on a Carlo Erba 1108 elemental analyzer and a PerkinElmer 2400 elemental analyzer by Atlantic Microlabs, Inc.

2.3. Proton nuclear magnetic resonance

^{1}H NMR spectra were collected using a 400 MHz Varian MR400 or 500 MHz Varian vnmrs 500 spectrometer. Solutions were prepared in d_6-DMSO or d_4-MeOH and collected using a standard pulse sequence for 45° excitation. Spectra were processed using MestraNOVA 6.0 software.

2.4. ^1H–^1H COSY

COSY experiments were performed in a mixture of 9:1 d_4-MeOH and d_6-DMSO using a 500 MHz Varian vnmrs 500 spectrometer using a standard pulse sequence with 16 scans using 128 T_1 increments. Spectra were processed using MestraNOVA 6.0 software.

2.5. X-ray crystallography

Colorless plates of **Sm-e8** were grown from a *N*,*N*-dimethylformamide solution of the compound at ambient conditions. A crystal of dimensions 0.17 × 0.15 × 0.15 mm was mounted on a Rigaku AFC10K Saturn 944+ CCD-based X-ray diffractometer equipped with a low temperature device and Micromax-007HF Cu-target micro-focus rotating anode (λ = 1.54187 Å) operated at 1.2 kW power (40 kV, 30 mA). The X-ray intensities were measured at 85(1) K with the detector placed at a distance 42.00 mm from the crystal. A total of 2028 images were collected with an oscillation width of 1.0° in ω. The exposure times were 1 s. for the low angle images, 3 s. for high angle. Rigaku d*trek images were exported to CrysAlisPro for processing and corrected for absorption [38]. The integration of the data yielded a total of 151,350 reflections to a maximum 2θ value of 69.55° of which 18,269 were independent and 17,636 were greater than 2σ(I). The final cell constants (Table S1) were based on the xyz centroids of 71,740 reflections above 10σ(I). Analysis of the data showed negligible decay during data collection. The structure was solved and refined with the Bruker SHELXTL (version 2018/3) software package [39], using the space group $P2_1/n$ with Z = 2 for the formula $C_{137.6}H_{140.4}Ga_8N_{19.2}Na_2O_{64.2}Sm_2$. All non-hydrogen atoms were refined anisotropically with the hydrogen atoms placed in idealized positions, with the exception of H21A, H21B, H22A, H22B, H23A, H23B, H24A, H24B which were refined from the difference map using DFIX and DANG restraints. Full matrix least-squares refinement based on F^2 converged at R1 = 0.0555 and wR2 = 0.1680 [based on $I > 2$sigma (I)], R1 = 0.0568 and wR2 = 0.1700 for all data. The SQUEEZE subroutine of the PLATON program suite was used to address the disordered solvent present in the structure [40]. Additional details are presented in Table S1 and are given as Supporting Information in a CIF file.

2.6. Absorption spectroscopy

Solution-state UV–vis spectra were collected on samples dissolved in methanol or a 9:1 mixture of methanol and DMF (approx. 100 µM) using a Cary 100Bio UV–Vis spectrophotometer in absorbance mode. Extinction coefficients were determined using the Beer-Lambert law by measuring five serial additions of the 100 mM stock to 3 mL of methanol. Data were processed using Microsoft Excel 2013 and SigmaPlot 10 software.

2.7. Solution-state fluorescence spectroscopy

Approximately 2 µM solutions of metallacrown were prepared and measured for solution state excitation and emission using a Horiba Scientific Fluoromax 4 fluorimeter in a 1 mL quartz cuvette. Excitation spectra were measured using a λ_{em} of 595 nm and a slit width of 2 nm for the excitation and a slit width of 5 nm for the emission. Emission spectra were recorded using a λ_{ex} of 315 nm for **Sm-m4** and **Sm-te4** or λ_{ex} of 340 nm for **Sm-e8** and **Sm-bt8** with an excitation slit width of 5 nm and an emission slit width of 2 nm. Background spectra of methanol were recorded and used to subtract second harmonic artifacts. Data were processed using Origin 8 and SigmaPlot 10 software.

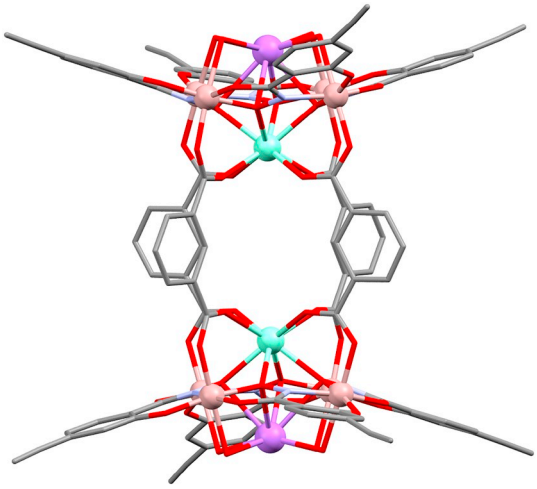

Fig. 1. X-ray crystal structure of **Sm-e8**. Solvent molecules and hydrogen atoms are removed for clarity. The color scheme for atoms is the following: Sm = green; Na = purple, C = grey, N = blue, O = red.

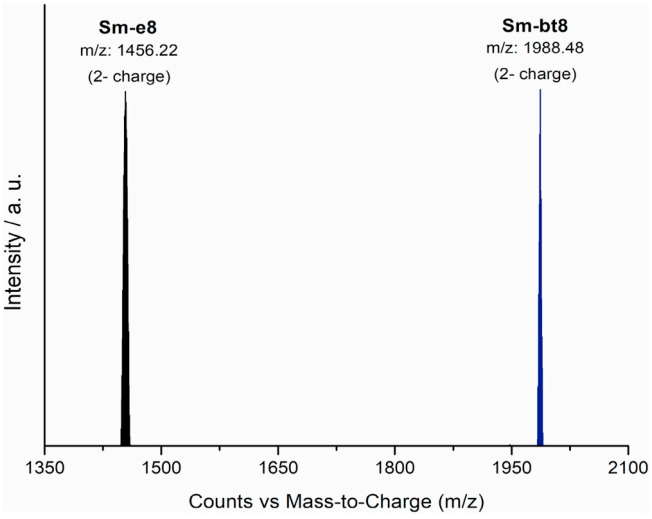

Fig. 2. ESI-MS of the fully coupled **Sm-bt8** with eight benzyl azides. The spectrum was collected in methanol in negative ion mode with a fragmentation voltage of 250 V. The background spectrum was not subtracted.

3. Results and discussion

3.1. Synthesis and structure

Stoichiometric addition of the metallacrown components results in desired coordination complexes with samarium or yttrium. Consistent ESI-MS, elemental analysis, and ^{1}H NMR demonstrate the formation of a consistent composition of either $\{Ln[12\text{-}MC^{III}_{GaN(eshi)}\text{-}4]\}_2(iph)_4$ or $\{Ln[12\text{-}MC^{III}_{GaN(shi)}\text{-}4]\}_2(miph)_4$ for each respective lanthanide (Fig. 2, Fig. 3, and Figs. S7–10, Supporting Information). **Sm-e8** crystallized in the space group $P2_1/n$ from slow evaporation of DMF and the resulting structure is shown in Fig. 1. The overall structure is reminiscent of a previously reported $\{Dy[12\text{-}MC^{III}_{GaN(shi)}\text{-}4]\}_2(iph)_4$ metallacrown [18] except that the shi^{3-} hydroximate is now $eshi^{3-}$ and sodium counter-cations were used instead of the ammonium ions in the original structure. The samarium(III) are eight-coordinate where four oxime oxygens from the metallacrown comprise one face of a distorted square antiprism and four carboxylate oxygens bind from the isophthalate ligands to form the other. The gallium ions are in six-coordinate pseudo-octahedral geometry where the equatorial positions are occupied by the metallacrown chelate motif from the hydroximates, one axial position is filled by a carboxylate oxygen on isophthalate, and the other axial site is coordinated to a solvent molecule. The sodium counter cations are also incorporated into the solid state structure on the opposite face of the metallacrown from the samarium in a nine-coordinate monocapped square antiprism geometry, where four sites are occupied by metallacrown oxime oxygens, four are filled by solvents, and the final apical position is filled by a solvent with 50% occupancy. This sodium binding motif has been observed in two previously reported metallacrowns using gallium(III) or manganese(III) [41,42].

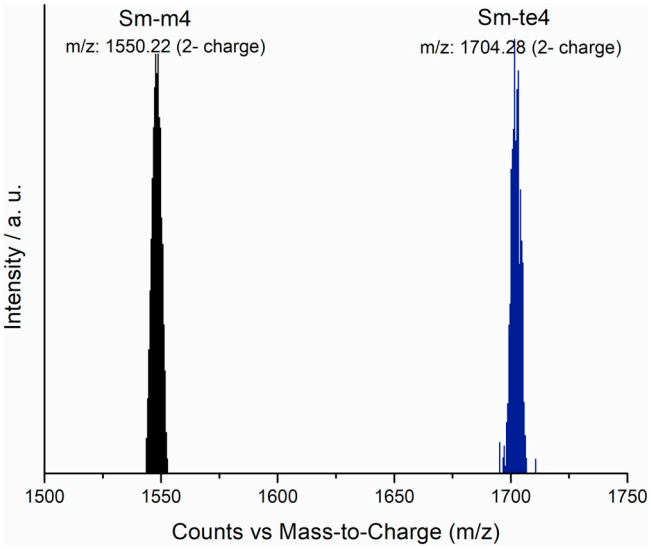

Fig. 3. ESI-MS of the fully coupled **Sm-te4** with four cysteamine. The spectrum was collected in methanol in negative ion mode with a fragmentation voltage of 250 V. The background spectrum was subtracted once.

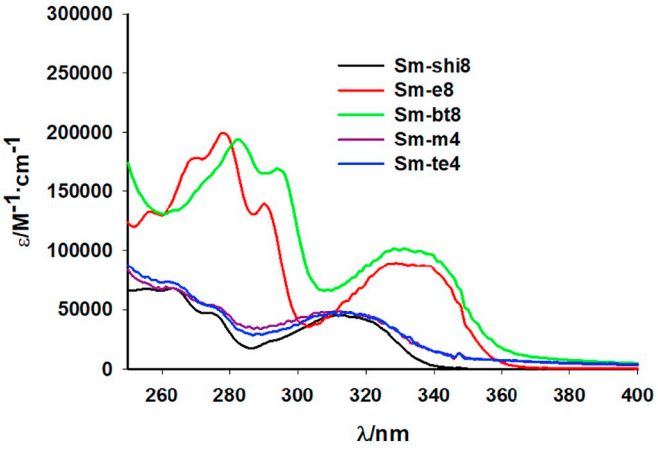

Fig. 4. UV–Vis absorbance of samarium metallacrown complexes in approx. 2–3 μM methanol solution at room temperature.

Solution state composition was determined from consistent ESI-MS and ^{1}H NMR for the Sm^{3+} and Y^{3+} analogs in methanol solutions. ESI-MS shows spectra with only one peak present with a − 2 charge of consistent mass for the metallacrown moiety (Fig. S1, Supporting Information). **Sm-e8**, **Y-e8, Sm-m4** and **Y-m4** have ^{1}H NMR spectra consistent with a fourfold symmetric complex where integration gives a two to one ratio between the iph^{2-} and the shi^{3-} derivatives (Figs. S7–10, Supporting Information). The peak assignment was confirmed using COSY for **Y-e8** and **Y-m4**, where expected correlations between peaks related to the salicylhydroximate or the isophthalate are observed for each ligand (Figs. S11 and S12, Supporting Information). Taken together, the observation of a single peak in ESI-MS and well defined ^{1}H NMR spectra suggest that the complex is solution stable. To confirm the

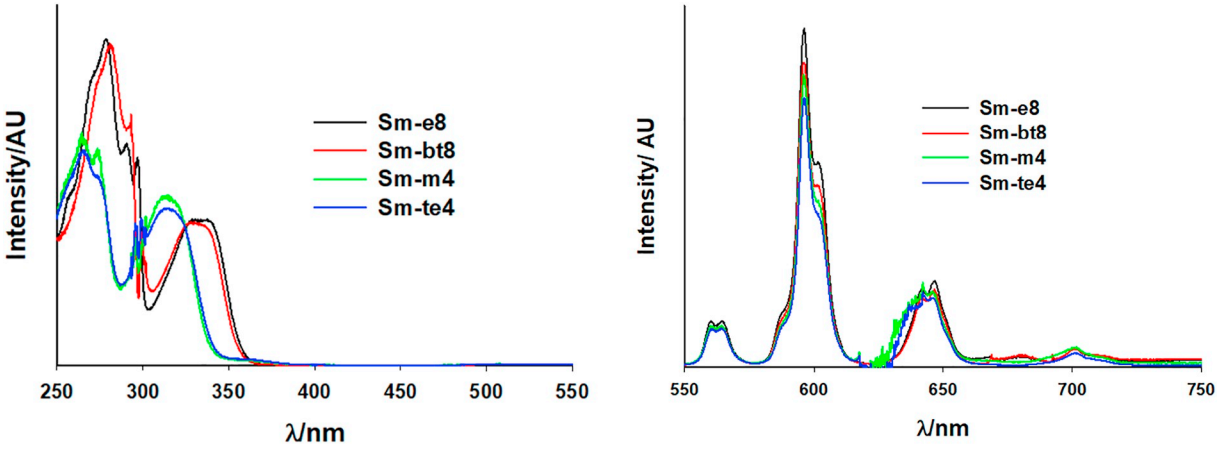

Fig. 5. Solution state excitation (λ_{em} = 595 nm, left) and emission (λ_{ex} = 315 or 340 nm, right) spectra of samarium metallacrowns collected in approx. 2 μM solutions at room temperature. Background spectra were subtracted to remove second harmonic artifacts.

long term stability of these metallacrowns ESI-MS in methanol (Fig. S13) was performed. Both **Y-m4** and the yttrium analog of the previously reported unmodified metallacrown dimer were dissolved in the same solution, which was monitored over the course of five days. After five days both peaks are still observed as discrete species, suggesting there is no exchange of ligands.

3.2. Coupling of small molecules to a metallacrown

The CuAAC reaction was carried out as described in the experimental section above to isolate a grey solid. ESI-MS on this recovered solid shows a − 2 peak at 1986.94 *m/z* which is consistent with complete conversion of the ethnyne to a benzyl triazole on **Sm-e8** (Fig. 2). This result demonstrates that it is possible to transfer the CuAAC method reported by Rentschler and coworkers onto non-cupric metallacrown scaffolds without altering the metallacrown by replacing either gallium or lanthanide ions with copper ions.

The Michael Addition was carried out on a maleimido functionality on the isophthalate bridge to form a thioether linkage as described in the experimental section above. Four cysteamine molecules were appended to the metallacrown demonstrating a complete conversion of the maleimide to a succinamide thioether. ESI-MS shows a single peak at 1702.18 *m/z* which corresponds to the complete conversion of all four malimido functional groups to a coupled thioether with cysteamine (Fig. 3).

These results highlight two interesting ideas. The first is that one may incorporate the capability to couple molecules of interest to these metallacrown species using either an ethynyl functionality or a maleimido functionality. The second is that since these functional groups are either on the hydroximate or the carboxylate ligand of the metallacrown, one may strive for orthogonal functionality where the CuAAC reaction may lead to coupling of one molecule, while the maleimido could couple another molecule independently of one another, all on the same metallacrown scaffold.

3.3. Optical properties

The reported {Sm[12-MC$_{GaN(shi)}^{III}$-4]}$_2$(iph)$_4$ metallacrown was synthesized according to the published procedure and used as a basis of comparison [18]. The solution state absorbance of **Sm-e8**, **Sm-m4**, **Sm-bt8** and **Sm-te4** analogs was measured in methanol solutions. The absorbance spectrum for each analog shown in Fig. 4 have a π-π* transition band with λ_{max} of approximately 315 nm (31,750 cm^{-1}) or 335 nm (29,850 cm^{-1}). This π-π* transition is red-shifted by close to 25 nm from the original shi^{3-} metallacrown in the case of **Sm-e8** and **Sm-bt8**. The redshift in this band also shows a redshift in the S_1 energy determined as the absorbance edge from 340 nm to 370 nm. There is no notable redshift in this absorbance for **Sm-m4** or **Sm-te4**. Solution-state excitation and emission spectra were also determined for the samarium metallacrowns. The extinction coefficients do not appreciably change after coupling is performed on the metallacrown. Characteristic Sm^{3+} emission bands are observed with bands at 560 nm ($^4G_{5/2}$ ➔$^6H_{5/2}$), 595 nm ($^4G_{5/2}$ ➔$^6H_{7/2}$), 645 nm ($^4G_{5/2}$ ➔$^6H_{9/2}$), and 700 nm ($^4G_{5/2}$ ➔$^6H_{11/2}$) (Fig. 5). The excitation spectrum (Fig. 5) shows a smooth region between 250 and 360 nm indicative of an antenna effect sensitization for **Sm-e8** and **Sm-bt8**, while **Sm-m4** and **Sm-te4** show sensitization between 250 nm and 345 nm. The antenna effect region edge is redshifted by approximately 15 nm between the two spectroscopic profiles. It also important to note that the capability to sensitize samarium is preserved after coupling a small molecule to the metallacrown.

4. Conclusions

The tunable nature of metallacrown scaffolds was exploited to incorporate an ethynyl and a maleimido functionality onto a known metallacrown structure in a controlled fashion. The eshi^{3-} ligand was able to operate as an antenna for lanthanide sensitization where both the UV–vis absorbance and excitation spectra show a significant redshift compared to the original shi^{3-} metallacrown. The ethynyl group was coupled to benzyl azide to fully convert **Sm-e8** from eight ethynyes to 8 benzyl triazoles and was confirmed using mass spectrometry. Similarly, the conversion of a maleimido to a thioether was shown on **Sm-m4** using cysteamine. The ability to sensitize samarium is preserved after each coupling is accomplished indicating that this could be a useful route for coupling other organic azides or thiol-bearing molecules of interest to a luminescent metallacrown complex.

Acknowledgements

This work was funded by the National Science Foundation [CHE-1664964 and CHE-0840456]. The authors declare no conflicts of interest.

Appendix A. Supplementary data

Supplementary data to this article can be found online at https://doi.org/10.1016/j.jinorgbio.2018.12.011.

References

[1] M.S. Lah, V.L. Pecoraro, Isolation and characterization of

{$Mn^{II}[Mn^{III}$(salicylhydroimate)]$_4$(acetate)$_2$(DMF)$_6$}·2DMF: an inorganic analogue of M^{2+}(12-crown-4), J. Am. Chem. Soc. 111 (1989) 7258–7259.
[2] C.-S. Lim, J. Jankolovits, J.W. Kampf, V.L. Pecoraro, Chiral metallacrown supramolecular compartments that template nanochannels: self-assembly and guest absorption, Chem. Asian J. 5 (2010) 46–49, https://doi.org/10.1002/asia.200900612.
[3] J.T. Grant, J. Jankolovits, V.L. Pecoraro, Enhanced guest affinity and enantioselectivity through variation of the Gd 3+ [15-metallacrown-5] side chain, Inorg. Chem. 51 (2012) 8034–8041, https://doi.org/10.1021/ic300110g.
[4] J. Jankolovits, C.-S. Lim, G. Mezei, J.W. Kampf, V.L. Pecoraro, Influencing the size and anion selectivity of dimeric ln 3+ [15-metallacrown-5] compartments through systematic variation of the host side chains and central metal, Inorg. Chem. 51 (2012) 4527–4538, https://doi.org/10.1021/ic202347j.
[5] C.-S. Lim, J. Jankolovits, P. Zhao, J.W. Kampf, V.L. Pecoraro, Gd(III)[15-METALLACROWN-5] recognition of chiral α-amino acid analogues, Inorg. Chem. 50 (2011) 4832–4841, https://doi.org/10.1021/ic102579t.
[6] T.T. Boron, J.C. Lutter, C.I. Daly, C.Y. Chow, A.H. Davis, A. Nimthong-Roldán, M. Zeller, J.W. Kampf, C.M. Zaleski, V.L. Pecoraro, The nature of the bridging anion controls the single-molecule magnetic properties of DyX 4 M 12-metallacrown-4 complexes, Inorg. Chem. 55 (2016) 10597–10607, https://doi.org/10.1021/acs.inorgchem.6b01832.
[7] C.M. Zaleski, S. Tricard, E.C. Depperman, W. Wernsdorfer, T. Mallah, M.L. Kirk, V.L. Pecoraro, Single molecule magnet behavior of a pentanuclear Mn-based metallacrown complex: solid state and solution magnetic studies, Inorg. Chem. 50 (2011) 11348–11352, https://doi.org/10.1021/ic2008792.
[8] C.Y. Chow, R. Guillot, E. Rivière, J.W. Kampf, T. Mallah, V.L. Pecoraro, Synthesis and magnetic characterization of Fe(III)-based 9-metallacrown-3 complexes which exhibit magnetorefrigerant properties, Inorg. Chem. 55 (2016) 10238–10247, https://doi.org/10.1021/acs.inorgchem.6b01404.
[9] C.Y. Chow, H. Bolvin, V.E. Campbell, R. Guillot, J.W. Kampf, W. Wernsdorfer, F. Gendron, J. Autschbach, V.L. Pecoraro, T. Mallah, Assessing the exchange coupling in binuclear lanthanide(III) complexes and the slow relaxation of the magnetization in the antiferromagnetically coupled Dy_2 derivative, Chem. Sci. 6 (2015) 4148–4159, https://doi.org/10.1039/C5SC01029B.
[10] C. Atzeri, L. Marchiò, C.Y. Chow, J.W. Kampf, V.L. Pecoraro, M. Tegoni, Design of 2D porous coordination polymers based on metallacrown units, Chem. Eur. J. 22 (2016) 6482–6486, https://doi.org/10.1002/chem.201600562.
[11] K.A. Mengle, E.J. Longenecker, M. Zeller, C.M. Zaleski, One-dimensional coordination polymers of 12-metallacrown-4 complexes: {Na2(L)2[12- MC M n III (N) shi -4]} n, where L is either −O2CCH2CH3 or −O2CCH2CH2CH3, J. Chem. Crystallogr. 45 (2015) 36–43, https://doi.org/10.1007/s10870-014-0560-0.
[12] L. Croitor, E.B. Coropceanu, O. Petuhov, K.W. Krämer, S.G. Baca, S.-X. Liu, S. Decurtins, M.S. Fonari, A one-dimensional coordination polymer based on Cu3-oximato metallacrowns bridged by benzene-1,4-dicarboxylato ligands: structure and magnetic properties, Dalton Trans. 44 (2015) 7896–7902, https://doi.org/10.1039/c5dt00533g.
[13] M.S. Muravyeva, G.S. Zabrodina, M.A. Samsonov, E.A. Kluev, A.A. Khrapichev, M.A. Katkova, I.V. Mukhina, Water-soluble tetraaqua Ln (III) glycinehydroximate 15-metallacrown-5 complexes towards potential MRI contrast agents for ultra-high magnetic field, Polyhedron 114 (2016) 165–171, https://doi.org/10.1016/j.poly.2015.11.033.
[14] A.J. Stemmler, J.W. Kampf, M.L. Kirk, B.H. Atasi, V.L. Pecoraro, The preparation, characterization, and magnetism of copper 15-metallacrown-5 lanthanide complexes, Inorg. Chem. 38 (1999) 2807–2817, https://doi.org/10.1021/ic9800233.
[15] E.R. Trivedi, S.V. Eliseeva, J. Jankolovits, M.M. Olmstead, S. Petoud, V.L. Pecoraro, Highly emitting near-infrared lanthanide “Encapsulated Sandwich” metallacrown complexes with excitation shifted toward lower energy, J. Am. Chem. Soc. 136 (2014) 1526–1534, https://doi.org/10.1021/ja4113337.
[16] J. Jankolovits, C.M. Andolina, J.W. Kampf, K.N. Raymond, V.L. Pecoraro, Assembly of near-infrared luminescent lanthanide host(host-guest) complexes with a metallacrown sandwich motif, Angew. Chem. Int. Ed. 50 (2011) 9660–9664, https://doi.org/10.1002/anie.201103851.
[17] C.Y. Chow, S.V. Eliseeva, E.R. Trivedi, T.N. Nguyen, J.W. Kampf, S. Petoud, V.L. Pecoraro, Ga 3+/Ln 3+ metallacrowns: a promising family of highly luminescent lanthanide complexes that covers visible and near-infrared domains, J. Am. Chem. Soc. 138 (2016) 5100–5109, https://doi.org/10.1021/jacs.6b00984.
[18] T.N. Nguyen, C.Y. Chow, S.V. Eliseeva, E.R. Trivedi, J.W. Kampf, I. Martinić, S. Petoud, V.L. Pecoraro, One-step assembly of visible and near-infrared emitting metallacrown dimers using a bifunctional linker, Chem. Eur. J. 24 (2018) 1031–1035, https://doi.org/10.1002/chem.201703911.
[19] I. Martinić, S.V. Eliseeva, T.N. Nguyen, F. Foucher, D. Gosset, F. Westall, V.L. Pecoraro, S. Petoud, Near-infrared luminescent metallacrowns for combined in vitro cell fixation and counter staining, Chem. Sci. 8 (2017) 6042–6050, https://doi.org/10.1039/C7SC01872J.
[20] I. Martinić, S.V. Eliseeva, T.N. Nguyen, V.L. Pecoraro, S. Petoud, Near-infrared optical imaging of necrotic cells by photostable lanthanide-based metallacrowns, J. Am. Chem. Soc. 139 (2017) 8388–8391, https://doi.org/10.1021/jacs.7b01587.
[21] J.C. Lutter, S.V. Eliseeva, J.W. Kampf, S. Petoud, V.L. Pecoraro, A unique ln III {[3.3.1]Ga III metallacryptate} series that possesses properties of slow magnetic relaxation and visible/near-infrared luminescence, Chem. Eur. J. 24 (2018) 10773–10783, https://doi.org/10.1002/chem.201801355.
[22] G. Mezei, C.M. Zaleski, V.L. Pecoraro, Structural and functional evolutions of metallacrowns, Chem. Rev. 107 (2007) 4933–5003, https://doi.org/10.1021/cr078200h.
[23] C.Y. Chow, E.R. Trivedi, V. Pecoraro, C.M. Zaleski, Heterometallic mixed *3d-4f* metallacrowns: structural versatility, luminescence, and molecular magnetism, Comments Inorg. Chem. 35 (2015) 214–253, https://doi.org/10.1080/02603594.2014.981811.
[24] J.C. Lutter, C.M. Zaleski, V.L. Pecoraro, Metallacrowns: supramolecular constructs with potential in extended solids, solution-state dynamics, molecular magnetism, and imaging, in: R. van Eldik, R. Puchta (Eds.), Adv. Inorg. Chem. Vol 71 Supramol. Chem, Elsevier, 2018, pp. 177–246, , https://doi.org/10.1016/bs.adioch.2017.11.007.
[25] T.N. Nguyen, V.L. Pecoraro, Metallacrowns: from discovery to potential applications in biomolecular imaging, Compr. Supramol. Chem. II, 5th ed., Elsevier, 2017, pp. 195–212, , https://doi.org/10.1016/B978-0-12-409547-2.12543-0.
[26] J.-C.G. Bünzli, Lanthanide luminescence for biomedical analyses and imaging, Chem. Rev. 110 (2010) 2729–2755, https://doi.org/10.1021/cr900362e.
[27] J.-C.G. Bünzli, S.V. Eliseeva, Basics of lanthanide photophysics, in: P. Hanninen, H. Harma (Eds.), Lanthan. Lumin. Photophysical, Anal. Biol. Asp, Springer, Berlin, 2011, pp. 1–45, , https://doi.org/10.1007/4243.
[28] H.C. Kolb, M.G. Finn, K.B. Sharpless, Click chemistry: diverse chemical function from a few good reactions, Angew. Chem. Int. Ed. 40 (2001) 2004–2021, https://doi.org/10.1002/1521-3773(20010601)40:11<2004::AID-ANIE2004>3.0.CO;2-5.
[29] R. Huisgen, 1,3-Dipolar cycloadditions, Proc. Chem. Soc. (1961) 357–396, https://doi.org/10.1039/ps9610000357.
[30] M. Meldal, C.W. Tornøe, Cu-catalyzed azide−alkyne cycloaddition, Chem. Rev. 108 (2008) 2952–3015, https://doi.org/10.1021/cr0783479.
[31] Q. Wang, T.R. Chan, R. Hilgraf, V.V. Fokin, K.B. Sharpless, M.G. Finn, Bioconjugation by copper(I)-catalyzed azide-alkyne [3 + 2] cycloaddition, J. Am. Chem. Soc. 125 (2003) 3192–3193, https://doi.org/10.1021/ja021381e.
[32] B.H. Northrop, S.H. Frayne, U. Choudhary, Thiol–maleimide “click” chemistry: evaluating the influence of solvent, initiator, and thiol on the reaction mechanism, kinetics, and selectivity, Polym. Chem. 6 (2015) 3415, https://doi.org/10.1039/c5py00168d.
[33] J.R. Winther, C. Thorpe, Quantification of thiols and disulfides, Biochim. Biophys. Acta, Gen. Subj. 1840 (2014) 838–846, https://doi.org/10.1016/j.bbagen.2013.03.031.
[34] G.T. Hermanson, G.T. Hermanson, Introduction to bioconjugation, Bioconjugate Tech, Elsevier, 2013, pp. 1–125, , https://doi.org/10.1016/B978-0-12-382239-0.00001-7.
[35] A.B. Lowe, Thiol-ene “click” reactions and recent applications in polymer and materials synthesis, Polym. Chem. 1 (2010) 17–36, https://doi.org/10.1039/B9PY00216B.
[36] C. Plenk, J. Krause, M. Beck, E. Rentschler, Rational linkage of magnetic molecules using click chemistry, Chem. Commun. 51 (2015) 6524–6527, https://doi.org/10.1039/C5CC00595G.
[37] E.R. Trivedi, V.L. Pecoraro, S.V. Eliseeva, S. Petoud, C.Y. Chow, T.N. Nguyen, J.C. Lutter, I. Martinic, Ln(III) and Ga(III) Metallacrown Complexes, WO 2016-EP58587, (2016).
[38] CrysAlisPro, 1.171.38.41 (Rigaku Oxford Diffraction), (2015).
[39] G.M. Sheldrick, Crystal structure refinement with SHELXL, Acta Crystallogr. Sect. C: Struct. Chem. 71 (2015) 3–8, https://doi.org/10.1107/S2053229614024218.
[40] A.L. Spek, PLATON SQUEEZE: a tool for the calculation of the disordered solvent contribution to the calculated structure factors, Acta Crystallogr. Sect. C: Struct. Chem. 71 (2015) 9–18, https://doi.org/10.1107/S2053229614024929.
[41] M.S. Lah, B.R. Gibney, D.L. Tierney, J.E. Penner-Hahn, V.L. Pecoraro, The fused metallacrown anion Na2{[Na0.5[Ga(salicylhydroximate)]4]2(.mu.2-OH)4}- is an inorganic analog of a cryptate, J. Am. Chem. Soc. 115 (1993) 5857–5858, https://doi.org/10.1021/ja00066a077.
[42] M.R. Azar, T.T. Boron, J.C. Lutter, C.I. Daly, K.A. Zegalia, R. Nimthong, G.M. Ferrence, M. Zeller, J.W. Kampf, V.L. Pecoraro, C.M. Zaleski, Controllable formation of heterotrimetallic coordination compounds: systematically incorporating lanthanide and alkali metal ions into the manganese 12-metallacrown-4 framework, Inorg. Chem. 53 (2014) 1729–1742, https://doi.org/10.1021/ic402865p.